

Received April 27, 2020, accepted May 24, 2020, date of publication May 27, 2020, date of current version June 8, 2020.

Digital Object Identifier 10.1109/ACCESS.2020.2997941

# Variational Mode Decomposition-Based Threat Classification for Fiber Optic Distributed Acoustic Sensing

SALEH A. ABUFANA<sup>1</sup>, YASER DALVEREN<sup>2,3</sup>, ALGHANNAI AGHNAIYA<sup>4</sup>,  
AND ALI KARA<sup>1</sup>, (Senior Member, IEEE)

<sup>1</sup>Department of Electrical and Electronics Engineering, Atilim University, 06830 Ankara, Turkey

<sup>2</sup>Department of Electronic Systems, Faculty of Information Technology and Electrical Engineering, Norwegian University of Science and Technology, 2815 Gjøvik, Norway

<sup>3</sup>Department of Avionics, Atilim University, 06830 Ankara, Turkey

<sup>4</sup>Department of Communications Engineering, College of Electronics Technology, Bani Waled, Libya

Corresponding author: Yaser Dalveren (yaser.dalveren@ntnu.no)

**ABSTRACT** In this study, a novel method is proposed to detect and classify the threats for fiber optic distributed acoustic sensing (DAS) systems. In the study, phase-sensitive optical time-domain reflectometry (phase-OTDR) is realized for the sensing system. The proposed method is consisted of three main stages. In the first stage, Wavelet denoising method is applied for noise reduction in the measured signal, and difference in time domain approach is used to perform high-pass filtering. Autocorrelation is then used for comparing the signal with itself over time in each bin to remove uncorrelated signals. Next, the power of the correlated signals at each bin is calculated and sorted where maximum valued bins are considered as the event signal. In the second stage, Variational Mode Decomposition (VMD) technique is used to decompose the detected event signals into a series of band-limited modes from which the event signals are reconstructed. From the reconstructed event signals, higher order statistical (HOS) features including variance, skewness, and kurtosis are extracted. In the last stage, the threats are discriminated by implementing Linear Support Vector Machine (LSVM)-based classification approach to the extracted features. In order to evaluate the effects of proposed method on the classification performance, different types of activities such as digging with hammer, pickaxe, and shovel collected from various points of a buried fiber optic cable have been used under different Signal-to-Noise Ratio (SNR) levels (−4 to −18 dB). It has observed that the classification accuracy at high/moderate (−4 to −8 dB) and low (−8 to −18 dB) SNR levels are 79.5% and 75.2%, respectively. To the best of authors' knowledge, this research study is the first report to use VMD technique for threat classification in phase-OTDR-based DAS systems.

**INDEX TERMS** Distributed acoustic sensing, optical time-domain reflectometry, Rayleigh backscattering light, support vector machine, threat classification, variational mode decomposition.

## I. INTRODUCTION

In recent years, use of fiber optic distributed acoustic sensing (DAS) has been attracting intensive attention in the field of vibration detection. Basically, it is based on the measurement of Rayleigh scattering that occurs when the light travelling in fiber optic cable is backscattered due to imperfections (known as “scattering centers”) along the cable [1]. Theoretically, the mechanical vibrations due to the physical activities or events taken place around the cable cause fluctuations in

the backscattered light. Interrogating these fluctuations then enable to detect and classify such activities. In this context, phase-sensitive optical time-domain reflectometry (phase-OTDR) technique has been developed for DAS during the last two decades [2], [3]. Unlike conventional OTDR, in phase-OTDR, pulses of highly coherent lights are used to transmit into a fiber optic cable, and for this reason, it is sensitive to relative phases of reflected fields from the scattering centers. Hence, it provides an efficient way for the monitoring of multi-point acoustic vibrations along the cable. Its effectiveness has been demonstrated in various applications such as crack detection of structures [4], [5], railroad monitoring [6],

The associate editor coordinating the review of this manuscript and approving it for publication was Jun Shi<sup>1</sup>.

[7], traffic flow detection [8], vehicle detection [9], and intrusion detection [10]–[18].

It has already known that the backscattered signal sensed in a phase-OTDR based DAS system has generally quite low signal-to-noise ratio (SNR) which highly affects the vibration detection capability of the systems. Thus, several methods such as heterodyning [4], Fourier transforming [5], multi-dimension comprehensive analysis [7], polarization diversity detection [10], two-dimensional edge detection [11], Raman amplification [12], signal-noise separation [13], adaptive temporal/match filtering [14], [15], Wavelet denoising [6], [8], [9], [16], multi-scale permutation entropy and the zero-crossing rate [17], and difference in time-frequency domain [18] have been used to improve the threat/event detection performance. Although these methods provide promising results, it is still necessary to open new corridors in order to improve the quality of weak Rayleigh backscattered signal in event detection.

On the other hand, classifying physical events/threats constitutes an important stage of a phase-OTDR based DAS system which directly affects the system performance. Obviously, efficient techniques or approaches are required to achieve better classification accuracy. In this context, using advanced signal processing techniques can pave the way for improving the classification accuracy. One of the potential processing approaches could be an improved decomposition technique which is called as Variational Mode Decomposition (VMD) [19]. It is based on the concepts of Wiener filtering, analytic signal and frequency mixing or heterodyning. Due to its efficiency, it has been offered to apply in various applications including emitter identification [20], fluctuation analysis [21], and RF fingerprinting [22], [23]. So far, there is no evidence to use VMD technique in phase-OTDR-based DAS systems. Particularly, it can be employed to improve the accuracy of the features extracted from the detected event signals. Thus, with the help of the extracted features, it can be possible to achieve high classification accuracy.

In this study, it is aimed to propose an alternative method to detect and classify the threats for fiber optic DAS systems based on phase-OTDR. Unlike the other methods, this method uses Wavelet denoising, difference in time domain approach, and autocorrelation process together in event detection stage for the first time. Besides, to our best knowledge, this is the first method that uses VMD technique for threat classification. Basically, the proposed method is mainly consisted of three main stages. In the first stage of the proposed method, Wavelet denoising method is applied to remove the noise from the measured backscattered signal, and difference in time domain approach is used to perform high-pass filtering. In this stage, autocorrelation is also used for improving interferometric visibility of the events in all ranges (bins) along the fiber cable. Further, the power of the correlated signals at each bin is calculated and sorted. Hence, the maximum valued bins are considered to be the event signal. In the second stage, the detected event signals are decomposed into a series of band-limited modes by using VMD technique,

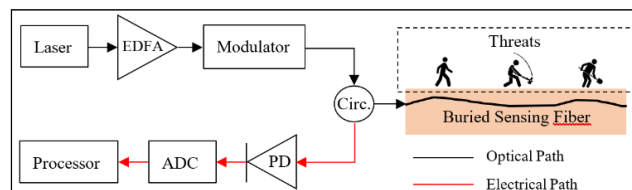


FIGURE 1. Phase-OTDR-based DAS system for threat detection.

and from these modes, the event signals are reconstructed. Moreover, from the reconstructed event signals, higher order statistical (HOS) features including variance, skewness, and kurtosis are extracted. In the last stage, Linear Support Vector Machine (LSVM)-based classification approach is implemented to the extracted features for discriminating the threats. In order to measure the effects of the proposed method on the classification performance, different types of activities collected from various points of a fiber optic cable have been used under different SNR levels. The results show the effectiveness of the proposed method in threat detection and classification.

The paper is organized as follows: In Section 2, the architecture of DAS system is overviewed. In Section 3, the proposed method is presented, and then experimental results are discussed to evaluate its overall performance. Lastly, in Section 4, conclusions are provided.

## II. A BRIEF OVERVIEW OF DISTRIBUTED ACOUSTIC SENSING (DAS) SYSTEM

A typical phase-OTDR-based DAS system for threat detection is shown in Fig. 1. Components of the illustrated system have been already well defined in several sources [10], [13], [18]. Fundamentally, light pulses emitted from a narrow line width ( $< 1$  kHz) continuous-wave (CW) laser source are amplified by an Erbium doped fiber amplifier (EDFA). The amplifier output is then sent to the acousto-optic modulator (AOM) which creates optical pulses before sending to buried sensing fiber by means of a circulator (Cir.). While travelling in the fiber, the optical pulse is exposed to Rayleigh scattering that causes a random intensity optical signal. When there is an external disturbance (typically vibrations on the ground nearby the fibre), the power of the Rayleigh backscattered signal generated from this external event is much larger than the background noise. The external disturbances (events) might be any vibration, such as walking, hitting, digging, etc. Time-frequency-energy variation of these disturbances induces phase changes on the backscattered light. Therefore, time-frequency energy characteristics of some expected events should be characterized well in order to develop a pattern recognition system. All these are discussed in detail in [24]. Next, the intensity of the optic lights modulated by these changes is easily detected by a photodetector (PD). The output of the PD is digitized using an analog-to-digital converter (ADC) to process the signal so that the threat can be detected, a direct detection approach using the backscattered light intensity directly is used without

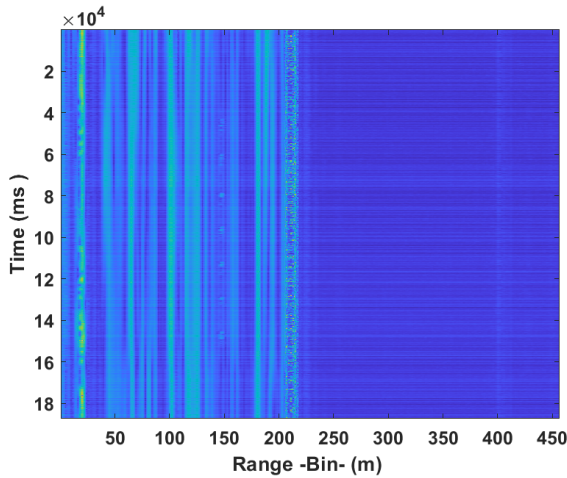


FIGURE 2. A raw DAS data.

any demodulation in this paper since it is easy to implement. However, in practice, it is not easy to extract a real event signal from the nonlinearly mixed signals. The proposed method that could be an alternative to alleviate this problem is presented in the following section.

### III. THE PROPOSED METHOD

As mentioned previously, the proposed method is mainly consisted of three main stages: a) Event detection, b) Event reconstruction and feature extraction, and c) Event classification. Details of these stages are provided in the following subsections.

#### A. STAGE I—EVENT DETECTION

In the first step of the event detection, backscattered signal due to external events ( $y(t)$ ) is needed to be extracted from the measured backscattered signal ( $x(t)$ ). Simply, the relationship between  $x(t)$  and  $y(t)$  can be expressed as

$$x(t) = y(t) + n(t) \tag{1}$$

where  $n(t)$  is considered as background noise that is typically presence in the cable due to thermal noise and cable characteristics. The aim is then to extract  $y(t)$  from  $x(t)$  by suppressing  $n(t)$ . To that end, the proposed method begins with removing noise from  $x(t)$  by applying Wavelet denoising method [16] to clean up the signal. Wavelets are able to localize signal features to different scales. Hence, while removing noise from the signal, it is possible to preserve significant signal features. It is already known that a large number of wavelets can be used for both continuous and discrete analysis. In this study, DAS data for each channel is decomposed at level 5 using sym5 symlet wavelets [18]. As an illustration, a raw data of manual digging activity with pickaxe and denoised data obtained by applying Wavelet denoising are shown in Fig. 2 and 3, respectively.

After applying Wavelet denoising, difference in time domain approach is used to implement high-pass filter and

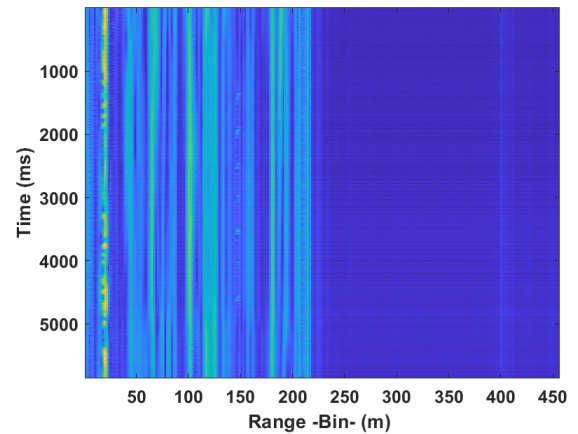


FIGURE 3. Denoised data.

also extract abrupt changes in the signal [18]. Before using this approach, the signal  $x(t)$  needs to be digitized:

$$x[c, m] = y[c, m] + n[c, m], \tag{2}$$

where  $c$  is the measurement point on the cable ( $c \in Z^+$ ), and  $m$  is the digital time index. The differencing in time domain between consecutive pulses can be then expressed as

$$\begin{aligned} x_d[c, m] &= x[c, m + 1] - x[c, m], \\ &= (y[c, m + 1] + n[c, m + 1]) - (y[c, m] + n[c, m]), \\ &= (y[c, m + 1] - y[c, m]) + (n[c, m + 1] - n[c, m]), \\ &= y_d[c, m] - n_d[c, m]. \end{aligned} \tag{3}$$

It should be noted that the differencing between consecutive pulses is relied on an assumption. According to this assumption, the background noise, due to external disturbance on the cable, does not change in a short time interval as opposed to Rayleigh backscattered signal. This case can be attributed to Parseval's relation which can be stated as

$$\sum_{m=0}^{N-1} |y_d[c, m]|^2 \gg \sum_{m=0}^{N-1} |n_d[c, m]|^2, \tag{4}$$

where  $N$  denotes the number of samples utilized in signal power estimation. Hence, in this method, a specific function to suppress the noise is not used. Obviously, only time domain differencing is used to perform high-pass filtering and extract abrupt changes. Fig. 4 shows a graphics illustrating difference in time domain approach for the denoised data obtained in Fig. 3.

As can be seen from the figure, although the events occurred in some bins can be recognized, further processes are required for improving interferometric visibility of the activities in all bins. In fact, as discussed in [18], it is necessary to apply time-domain low-pass filtering in order to remove high frequency components due to the noise which is amplified by high-pass filtering. Instead, in this study, autocorrelation is used for comparing the signal with a time-delayed version of itself in each bin. Indeed, this yields

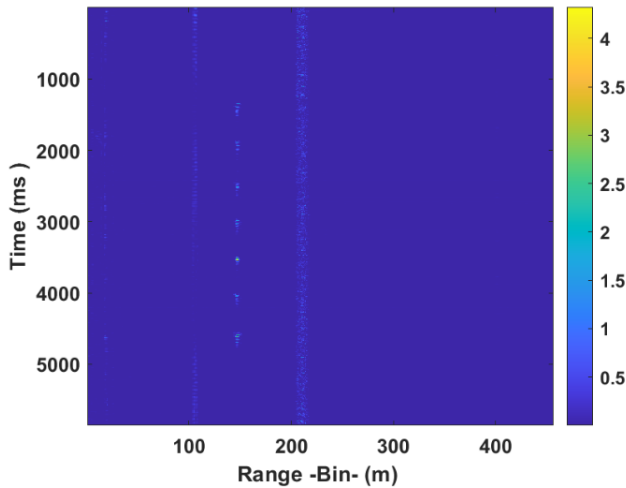


FIGURE 4. Difference in time domain approach applied on denoised data.

to comprehend the significant changes of the signals to reveal whether there is a significant relation between the signals or not. Theoretically, if  $N$  points are considered in time, the autocorrelation function  $R(c, \tau)$  for a discrete signal  $x_d[c, m]$  is calculated by [25], [26]

$$R(c, \tau) = \frac{1}{N} \sum_{m=1}^N x_d[c, m] x_d[c, m + \tau], \quad (5)$$

where  $\tau$  is lag number. Then, highly correlated signals ( $x_{dc}[m]$ ) exceeding a predefined threshold ( $\Gamma$ ) for each bin are decided:

$$x_{cor}[c, m] = \begin{cases} x_d[c, m], & R(c, \tau) > \Gamma \\ 0, & \text{otherwise} \end{cases} \quad (6)$$

Thus, unwanted (uncorrelated) signals are removed so that the bins where the events are occurred can be detected as shown in Fig. 5. When compared to Fig. 4, it is clear that the unwanted signals presence in bins between 200 – 250 is completely removed, and thus interferometric visibility of the activities occurred in bins between 10 – 150 is considerably improved.

In the last phase of the event detection, power of the correlated signals at each bin,  $P_x(c)$ , is calculated as

$$P_x(c) = \sum_{m=0}^{N-1} |x_{cor}[c, m]|^2. \quad (7)$$

Then, the corresponding values are sorted in a vector  $\mathbf{E}$  as

$$\mathbf{E} = \text{sort}\{P_x(c)\} \quad (8)$$

where  $\text{sort}\{\cdot\}$  denotes the *sorting* operator that sorts the values of  $P_x(c)$  in descending order as a sequence.

Finally, the maximum-valued bins are obtained by taking the maximum of the elements in  $\mathbf{E}$  ( $\max\{\mathbf{E}\}$ ). Therefore, the maximum-valued bins selected in  $\mathbf{E}$  correspond to the candidates of event detection. The signals observed at these bins are then considered as the event signals.

## B. STAGE II-EVENT RECONSTRUCTION AND FEATURE EXTRACTION

In this stage, the detected event signals are processed before classification. In fact, this stage has a vital importance in enhancing the detection performance of the system. Thus, the goal is to achieve robust features to be used in the event classification. To this end, the event signals detected from previous stage are decomposed and reconstructed, and then, HOS features are extracted from these reconstructed signals.

### 1) RECONSTRUCTION OF THE DETECTED EVENT SIGNALS

In order to reconstruct the event signals, VMD technique provided in [19] is utilized. Basically, it decomposes any real-valued signal  $s$  into a number of discrete modes  $s_z$  where  $z = 1, \dots, Z$ . These modes have specific properties for reproducing the input signal, and has also limited bandwidth in frequency domain where each of them compacts around a center frequency  $\omega_z$ . The bandwidth of a mode is evaluated as a specific norm of its Hilbert complemented. Then, by means of complex harmonic, the analytic signal is shifted. Alternate direction method of multipliers (ADMM) approach is used in order to solve the variational problem. Besides, to update the modes, Wiener filtering along with a filter are applied. Hence, each  $\omega_z$  is updated as the center of gravity of the  $s_z$  power spectrum. Therefore, the Lagrangian multiplier that enforces the reconstruction of the input signal is updated. Briefly, to create a mode, the following scheme is applied:

- The corresponding analytic signal for each mode is computed by Hilbert transform,
- Frequency spectrum of the mode is shifted to baseband by heterodyning,
- The bandwidth of the mode is estimated by smoothing the demodulated signal which is also known as Wiener filtering.

Thus, the constrained variational problem is written as

$$\min_{\{s_z\}, \{\omega_z\}} \left\{ \sum_z \left\| \partial_t \left[ \left( \delta(t) + \frac{j}{\pi t} \right) * s_z(t) \right] e^{-j\omega_z t} \right\|_2^2 \right\}, \quad (9)$$

$$s.t. \sum_z s_z = f.$$

The optimization problem is then transformed into an unconstrained form by introducing the augmented Lagrangian  $\mathcal{L}$ :

$$\begin{aligned} \mathcal{L}(\{s_z\}, \{\omega_z\}, \lambda) &= \alpha \sum_k \left\| \partial_t \left[ \left( \delta(t) + \frac{j}{\pi t} \right) * s_z(t) \right] e^{-j\omega_z t} \right\|_2^2 \\ &+ \left\| f(t) - \sum_k s_z(t) \right\|_2^2 + \langle \lambda(t), f(t) - \sum_k s_z(t) \rangle \\ &+ \langle \lambda(t), f(t) - \sum_k s_z(t) \rangle \end{aligned} \quad (10)$$

where  $\alpha$  is the balancing parameter, and  $\lambda$  is the Lagrangian multiplier. The solution for the problem in (10) is found by employing a sequence of iterative sub-optimizations which is

called as ADMM) To employ this method, subproblems with respect to  $s_z$  and  $\omega_z$  are required to solve. In this context,  $s_z$  is rewritten as a minimization problem such that:

$$\hat{s}_z^{n+1} = \arg \min \left\{ \alpha \left\| \partial_t \left[ \left( \delta(t) + \frac{j}{\pi t} \right) * s_z(t) \right] e^{-j\omega_z t} \right\|_2^2 + \left\| f(t) - \sum_i s_i(t) + \frac{\lambda(t)}{2} \right\|_2^2 \right\}. \quad (11)$$

After following the approaches given in [19], which are not stated here for the sake of simplicity, the resulting quadratic optimization problem can be written as in the following:

$$\hat{s}_z^{n+1} = \arg \min \left\{ \int_0^\infty 4\alpha (\omega - \omega_z)^2 |\hat{s}_z(\omega)|^2 + 2 \left| \hat{f}(\omega) - \sum_i \hat{s}_i(\omega) + \frac{\hat{\lambda}(\omega)}{2} \right|^2 d\omega \right\}. \quad (12)$$

The quadratic problem can be then solved by

$$\hat{s}_z^{n+1}(\omega) = \frac{\hat{f}(\omega) - \sum_{i \neq z} \hat{s}_i(\omega) + \frac{\hat{\lambda}(\omega)}{2}}{1 + 2\alpha (\omega - \omega_z)^2}. \quad (13)$$

As for the subproblem with respect to  $\omega_z$ , minimization problem is rewritten as:

$$\omega_z^{n+1} = \arg \min \left\{ \alpha \left\| \partial_t \left[ \left( \delta(t) + \frac{j}{\pi t} \right) * s_z(t) \right] e^{-j\omega_z t} \right\|_2^2 \right\} \quad (14)$$

which can be solved, after the problem is transformed into a quadratic problem given that the optimization takes place in Fourier domain, as

$$\omega_z^{n+1} = \frac{\int_0^\infty \omega |\hat{s}_z(\omega)|^2 d\omega}{\int_0^\infty |\hat{s}_z(\omega)|^2 d\omega}. \quad (15)$$

Therefore, by substituting the solutions given in (13) and (15) into the ADMM method, an algorithm for VMD can be achieved. It can be summarized as provided in the following procedure [22]:

- Set n to 0 for initializing the modes ( $\hat{s}_z^1$ ,  $\omega_z^1$ , and  $\hat{\lambda}_z^1$ )
- Update  $\hat{s}_z^{n+1}(\omega)$  provided in (13)
- Update  $\omega_z^{n+1}$  provided in (15)
- Update Lagrange multiplier:  $\hat{\lambda}^{n+1}(\omega) \leftarrow \hat{\lambda}^n(\omega) + \tau \left( \hat{f}(\omega) - \sum_z \hat{s}_z^{n+1}(\omega) \right)$  until the convergence  $\sum_z \left\| \hat{s}_z^{n+1} - \hat{s}_z^n \right\|_2^2$ .

## 2) FEATURE EXTRACTION

Once the event signals are reconstructed, the next step is to extract distinctive signal features from the reconstructed signals by exploiting instantaneous signal characteristics such as instantaneous amplitude  $a(n)$ , instantaneous frequency  $f(n)$ , and instantaneous phase  $\varnothing(n)$ . For a real-valued discrete

signal in time domain  $s(n)$ , the analytic signal  $s^a(n)$  can be expressed as

$$s^a(n) = s_I^a(n) + js_Q^a(n) \quad (16)$$

where  $I$  and  $Q$  are the in-phase and quadrature components, respectively. These components are given by  $s_I^a(n) = s(n)$ ,  $s_Q^a(n) = H\{s(n)\}$  where  $H\{\cdot\}$  denotes Hilbert Transform. Therefore, the instantaneous signal characteristics ( $a(n)$ ,  $\varnothing(n)$ ,  $f(n)$ ) can be calculated as

$$a(n) = \sqrt{(s_I^a(n))^2 + (s_Q^a(n))^2}, \quad (17)$$

$$\varnothing(n) = \tan^{-1} \left[ \frac{s_Q^a(n)}{s_I^a(n)} \right], \quad (18)$$

$$f(n) = \frac{1}{2\pi} \frac{\varnothing(n) - \varnothing(n-1)}{\Delta n}. \quad (19)$$

Further, the biases superimposed by the data collection system are removed. To do that, receiver-induced linear component of the instantaneous phase is eliminated, and all characteristics are normalized [22]. Then, three HOS features (skewness, kurtosis, and variance) are calculated from  $a(n)$ ,  $\varnothing(n)$ , and  $f(n)$ . Hence, a total of nine feature vectors are created to be used in event classification.

## C. STAGE III-EVENT CLASSIFICATION

In the event classification stage of the proposed method, it is aimed to measure the effects of the proposed method on the classification performance. Although several approaches or techniques have been proposed for classification purposes, it is still necessary to achieve accurate results in classification of the detected events especially under realistic noise conditions. To that end, in the following subsections, the procedure for creating data under different noise conditions is described, and the details of the classification method employed to identify the events are presented.

### 1) DATA CREATION

Three types of activity were recorded from different points of a buried fiber cable. These events are: (1) Digging with hammer, (2) Digging with pickaxe, (3) Digging with shovel. Different levels of the channel noise were then added randomly to the records. While doing this, three datasets for each event were created by varying SNR levels. The ranges for the SNR levels were defined as: (a) low SNR (-8 to -18 dB), (b) high/moderate SNR (-4 to -8 dB). At each SNR range, there were 120 samples for each event. It should be also noted that SNR values of each dataset are distributed in approximately Gaussian distribution.

### 2) CLASSIFICATION AND RESULTS

Before making classification, the feature sets created in *Stage II* are divided into training and test sets for each event. Here, the feature sets are trained in order to make a relationship between the feature sets and the events, whereas, the test sets are used for estimating the performance of the classifier.

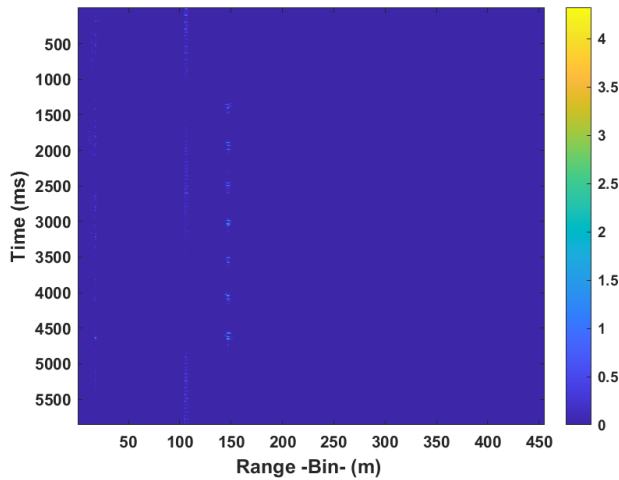


FIGURE 5. The detected bins where the events are occurred.

Output Class	1	49 23.3%	16 7.6%	5 2.4%	70.0% 30.0%
	2	19 9.0%	54 25.7%	10 4.8%	65.1% 34.9%
	3	2 1.0%	0 0.0%	55 26.2%	96.5% 3.5%
		70.0% 30.0%	77.1% 22.9%	78.6% 21.4%	75.2% 24.8%
		1	2	3	
		Target Class			

FIGURE 6. Confusion matrix for low SNR (−8 to −18 dB).

Output Class	1	45 21.4%	10 4.8%	2 1.0%	78.9% 21.1%
	2	15 7.1%	54 25.7%	0 0.0%	78.3% 21.7%
	3	10 4.8%	6 2.9%	68 32.4%	81.0% 19.0%
		64.3% 35.7%	77.1% 22.9%	97.1% 2.9%	79.5% 20.5%
		1	2	3	
		Target Class			

FIGURE 7. Confusion matrix for high/moderate SNR (−4 to −8 dB).

For classification, LSVM classifier has been employed due to its efficiency [22], [23]. Each training set consists of 70 (58%) out of 120 samples per event. The corresponding test set consists of the remaining 50 (42%) samples.

LSVM was trained with the training set, and its decision function was determined. The test set was then used to

measure the classification accuracy. The confusion matrices of the LSVM classifier for the datasets under low SNR and high/moderate SNR are shown in Fig. 6 and Fig. 7, respectively. In confusion matrices, the number and the percentage of misclassified samples are represented by red coloured cells while the number and the percentage of correctly classified samples are represented by green coloured cells.

When the confusion matrices are analysed, it is observed that the classification accuracy at high/moderate and low SNR levels are 79.5% and 75.2%, respectively. It is clear that the accuracy is decreased by ~4% under low SNR level. On the other hand, almost the same rates, 65.1% and 64.3%, are observed as the lowest classification accuracy at low and high/moderate SNR level, respectively.

#### IV. CONCLUSION

This paper presents a novel method to detect and classify the threats for phase-OTDR based fiber optic DAS systems. In the proposed method, threat detection is provided by a different approach which combines Wavelet denoising and difference in time domain methods with the autocorrelation process. For threat classification, on the other hand, VMD technique is used to extract HOS features (skewness, kurtosis, and variance) from the detected threats. In order to identify the threats, LSVM classifier is employed under different SNR levels. According to the classification performance results, it has obtained that the system becomes effective at identifying of physical activities such as digging with hammer, pickaxe, and shovel which are taken place around the buried fiber cable. More specifically, it has observed that better performance (~4% higher accuracy) could be achieved at higher SNR levels (−4 to −8 dB). But still, it has shown that acceptable classification performance (75.2%) could also be achieved at lower SNR levels (−8 to −18 dB).

#### REFERENCES

- [1] D. Hill, “Distributed acoustic sensing (DAS): Theory and applications,” in *Proc. Frontiers Opt.*, 2015, pp. 3–4.
- [2] Y. Wang, H. Yuan, X. Liu, Q. Bai, H. Zhang, Y. Gao, and B. Jin, “A comprehensive study of optical fiber acoustic sensing,” *IEEE Access*, vol. 7, pp. 85821–85837, 2019.
- [3] X. Liu, B. Jin, Q. Bai, Y. Wang, D. Wang, and Y. Wang, “Distributed fiber-optic sensors for vibration detection,” *Sensors*, vol. 16, no. 8, p. 1164, Jul. 2016.
- [4] Y. Lu, T. Zhu, L. Chen, and X. Bao, “Distributed vibration sensor based on coherent detection of phase-OTDR,” *J. Lightw. Technol.*, vol. 28, no. 22, pp. 3243–3249, Nov. 2010.
- [5] H. Yue, B. Zhang, Y. Wu, B. Zhao, J. Li, Z. Ou, and Y. Liu, “Simultaneous and signal-to-noise ratio enhancement extraction of vibration location and frequency information in phase-sensitive optical time domain reflectometry distributed sensing system,” *Opt. Eng.*, vol. 54, no. 4, Apr. 2015, Art. no. 047101.
- [6] F. Peng, N. Duan, Y.-J. Rao, and J. Li, “Real-time position and speed monitoring of trains using phase-sensitive OTDR,” *IEEE Photon. Technol. Lett.*, vol. 26, no. 20, pp. 2055–2057, Oct. 15, 2014.
- [7] Z. Wang, B. Lu, H. Zheng, Q. Ye, Z. Pan, H. Cai, R. Qu, Z. Fang, and H. Zhao, “Novel railway-subgrade vibration monitoring technology using phase-sensitive OTDR,” *Proc. SPIE*, vol. 10323, Apr. 2017, Art. no. 103237G.
- [8] H. Liu, J. Ma, W. Yan, W. Liu, X. Zhang, and C. Li, “Traffic flow detection using distributed fiber optic acoustic sensing,” *IEEE Access*, vol. 6, pp. 68968–68980, 2018.

- [9] H. Liu, J. Ma, T. Xu, W. Yan, L. Ma, and X. Zhang, "Vehicle detection and classification using distributed fiber optic acoustic sensing," *IEEE Trans. Veh. Technol.*, vol. 69, no. 2, pp. 1363–1374, Feb. 2020.
- [10] J. C. Juarez, E. W. Maier, K. Nam Choi, and H. F. Taylor, "Distributed fiber-optic intrusion sensor system," *J. Lightw. Technol.*, vol. 23, no. 6, pp. 2081–2087, Jun. 2005.
- [11] T. Zhu, X. Xiao, Q. He, and D. Diao, "Enhancement of SNR and spatial resolution in  $\phi$ -OTDR system by using two-dimensional edge detection method," *J. Lightw. Technol.*, vol. 31, no. 17, pp. 2851–2856, Sep. 2013.
- [12] F. Peng, H. Wu, X. Jia, Y. Rao, Z. Wang, and Z. Peng, "Ultra-long high-sensitivity-OTDR for high spatial resolution intrusion detection of pipelines," *Optic Express*, vol. 22, no. 11, pp. 13804–13810, Jun. 2014.
- [13] H. Wu, S. Xiao, X. Li, Z. Wang, J. Xu, and Y. Rao, "Separation and determination of the disturbing signals in phase-sensitive optical time domain reflectometry ( $\phi$ -OTDR)," *J. Lightw. Technol.*, vol. 33, no. 15, pp. 3156–3162, Aug. 1, 2015.
- [14] I. Ölçer and A. Öncü, "Adaptive temporal matched filtering for noise suppression in fiber optic distributed acoustic sensing," *Sensors*, vol. 17, no. 6, p. 1288, Jun. 2017.
- [15] M. Adeel, J. Tejedor, J. Macias-Guarasa, and C. Lu, "Improved perturbation detection in direct detected  $\phi$ -OTDR systems using matched filtering," *IEEE Photon. Technol. Lett.*, vol. 31, no. 21, pp. 1689–1692, Nov. 1, 2019.
- [16] Z. Qin, L. Chen, and X. Bao, "Wavelet denoising method for improving detection performance of distributed vibration sensor," *IEEE Photon. Technol. Lett.*, vol. 24, no. 7, pp. 542–544, Apr. 2012.
- [17] P. Ma, K. Liu, J. Jiang, Z. Li, P. Li, and T. Liu, "Probabilistic event discrimination algorithm for fiber optic perimeter security systems," *J. Lightw. Technol.*, vol. 36, no. 11, pp. 2069–2075, Jun. 1, 2018.
- [18] M. Aktas, T. Akgun, M. U. Demircin, and D. Buyukaydin, "Deep learning based multi-threat classification for phase-OTDR fiber optic distributed acoustic sensing applications," *Proc. SPIE*, vol. 10208, Apr. 2017, Art. no. 102080G.
- [19] K. Dragomiretskiy and D. Zosso, "Variational mode decomposition," *IEEE Trans. Signal Process.*, vol. 62, no. 3, pp. 531–534, Feb. 2014.
- [20] U. Satija, N. Trivedi, G. Biswal, and B. Ramkumar, "Specific emitter identification based on variational mode decomposition and spectral features in single hop and relaying scenarios," *IEEE Trans. Inf. Forensics Security*, vol. 14, no. 3, pp. 581–591, Mar. 2019.
- [21] Y. Liu, G. Yang, M. Li, and H. Yin, "Variational mode decomposition denoising combined the detrended fluctuation analysis," *Signal Process.*, vol. 125, pp. 349–364, Aug. 2016.
- [22] A. Aghnaiya, A. M. Ali, and A. Kara, "Variational mode decomposition-based radio frequency fingerprinting of Bluetooth devices," *IEEE Access*, vol. 7, pp. 144054–144058, 2019.
- [23] A. Aghnaiya, Y. Dalveren, and A. Kara, "On the performance of variational mode decomposition-based radio frequency fingerprinting of Bluetooth devices," *Sensors*, vol. 20, no. 6, p. 1704, Mar. 2020.
- [24] J. Tejedor, J. Macias-Guarasa, H. Martins, J. Pastor-Graells, P. Corredera, and S. Martin-Lopez, "Machine learning methods for pipeline surveillance systems based on distributed acoustic sensing: A review," *Appl. Sci.*, vol. 7, no. 8, p. 841, Aug. 2017.
- [25] S. Kay, "The effect of sampling rate on autocorrelation estimation," *IEEE Trans. Acoust., Speech, Signal Process.*, vol. ASSP-29, no. 4, pp. 859–867, Aug. 1981.
- [26] M. Rabuffetti, G. Scalera, and M. Ferrarin, "Effects of gait strategy and speed on regularity of locomotion assessed in healthy subjects using a multi-sensor method," *Sensors*, vol. 19, no. 3, p. 513, Jan. 2019.



**SALEH A. ABUFANA** was born in Bani Waled, Libya, in 1967. He received the B.Sc. degree in computer engineering from the College of Electronics Technology, Bani Waled, in 1992, and the M.Sc. degree in electrical and computer engineering from the Libyan Academy, Libya, in 2008. He is currently pursuing the Ph.D. degree with Atilim University, Turkey. His current research interest includes distributed acoustic sensing and its applications.



**YASER DALVEREN** was born in Ankara, Turkey, in 1985. He received the B.S., M.S., and Ph.D. degrees from Atilim University, Ankara, Turkey, in 2009, 2011, and 2016, respectively. He is currently pursuing the second Ph.D. degree with the Department of Electronic Systems, Norwegian University of Science and Technology (NTNU), Gjøvik. From 2009 to 2017, he was a Research Assistant with the Electrical and Electronics Engineering Department, Atilim University, where he has been an Assistant Professor with the Department of Avionics, since 2017. His research interests mainly include source localization, signal processing, wireless communications, and the Internet of Things.



**ALGHANNAI AGHNAIYA** was born in Bani Waled, Libya, in 1962. He received the B.Sc. degree in communications engineering from the College of Electronics Technology, Bani Waled, in 1993, the M.Sc. degree in communications engineering from Al-Mergib University, Libya, in 2007, and the Ph.D. degree from Atilim University, Turkey, in 2019. In 2008, he joined the Electrical and Electronics Engineering Department, College of Electronics Technology. He is currently with the College of Electronics Technology, where he is working as a Lecturer. His research interests include RF fingerprinting applications and image processing.



**ALI KARA** (Senior Member, IEEE) was born in Amasya, Turkey, in 1972. He received the degree in electronics engineering from Erciyes University, Kayseri, in 1992, the M.Sc. degree from Çukurova University, Adana, 1996, and the Ph.D. degree from Hacettepe University, Ankara, in 2002. He was with Polytechnic University (ECE), Brooklyn, NY, USA, from 1999 to 2000, where he conducted theoretical and experimental research as a Research Assistant in a project sponsored by Symbol Technologies (Motorola). He joined the Department of Electrical and Electronics Engineering, Atilim University, in 2000, and devoted himself to founding the Department. He is currently with Atilim University where he has been a Professor, since 2015, and also the Director of the Graduate School of Natural and Applied Sciences. He has published in refereed journals/conferences, and has led several projects in the areas of Radio Propagation, Virtual and Remote Laboratories (VRL), and Radar and Electronic Warfare Systems. In one of the projects, he led the group at Atilim University to develop a VRL platform on RF and communications (unique platform funded by the European Commission). On the other hand, he was with Tubitak Bilgem, as a Chief Researcher and a consultant on defense and security related projects, from 2006 to 2012. He is actively researching in areas of RF fingerprinting, locating, and identification of radio emitters, including radars and wireless devices, radio aspects of wireless communications, including channel modeling and antennas.

...